



LUND UNIVERSITY

Application of Cars Spectroscopy For Diagnostics In High-temperature Environment

Aldén, Marcus

Published in:
Kvantovaya Elektronika

DOI:
[10.1070/QE1988v018n06ABEH012283](https://doi.org/10.1070/QE1988v018n06ABEH012283)

1988

[Link to publication](#)

Citation for published version (APA):
Aldén, M. (1988). Application of Cars Spectroscopy For Diagnostics In High-temperature Environment. *Kvantovaya Elektronika*, 15(6), 1173-1184. <https://doi.org/10.1070/QE1988v018n06ABEH012283>

Total number of authors:
1

General rights

Unless other specific re-use rights are stated the following general rights apply:
Copyright and moral rights for the publications made accessible in the public portal are retained by the authors and/or other copyright owners and it is a condition of accessing publications that users recognise and abide by the legal requirements associated with these rights.

- Users may download and print one copy of any publication from the public portal for the purpose of private study or research.
- You may not further distribute the material or use it for any profit-making activity or commercial gain
- You may freely distribute the URL identifying the publication in the public portal

Read more about Creative commons licenses: <https://creativecommons.org/licenses/>

Take down policy

If you believe that this document breaches copyright please contact us providing details, and we will remove access to the work immediately and investigate your claim.

LUND UNIVERSITY

PO Box 117
221 00 Lund
+46 46-222 00 00

Application of CARS spectroscopy for diagnostics in high
temperature environment

Marcus Aldén

The Combustion Centre
Lund Institute of Technology
P.O. Box 118, S-221 00 Lund
Sweden

Invited paper at the IX Vavilov Conference on Nonlinear-Optics
Novosibirsk, USSR, 1987.

Application of CARS spectroscopy for diagnostics in high temperature
environment

Marcus Aldén

The Combustion Centre
Lund Institute of Technology
P.O. Box 118, S-221 00 Lund
Sweden

Abstract:

Different applications of Coherent anti-Stokes Raman Scattering (CARS) for non-intrusive diagnostics at high temperatures are reviewed. Its application to small laboratory flames and large-scale (10 x 10 m) furnaces are described as well as probing in electrical discharges. Finally the potential of using pure rotational CARS and its applicability to flame measurements are described.

I. Introduction

During the last two decades several laser spectroscopical techniques have been developed and applied in different areas for diagnostic purposes. One of the areas which has benefitted most from these new diagnostic techniques is the combustion field in which non-intrusive spatially and temporally resolved measurements are of great importance for a more complete picture of phenomena related to this field. One of the techniques that has proven to have a great potential for high temperature diagnostics is Coherent anti-Stokes Raman Scattering or CARS. The main advantages with CARS spectroscopy compared to e.g. spontaneous Raman Scattering (RS) for diagnostic purposes is the coherent nature of the CARS process and the signal strength, which could be on the order of 10^6 times stronger than RS. Another advantage with CARS over RS is that the CARS signal is generated in a spectral region where fluorescence, induced by the laser beams, is almost absent. This fact is of special importance when probing in sooty and particle laden environment where the weak RS is masked by broadband fluorescence from soot particles and large molecules.

The theory and first demonstration of this non-linear optical phenomenon was shown in the mid-sixties by Maker and Terhune [1], however, it was not until 1973 its application to combustion and high temperature diagnostics was proposed by Taran and coworkers [2]. Since this demonstration on H_2 molecules in a stable well defined H_2 /air flame, the technique has been used in several applications; see e.g. Refs. [3-10].

II. Brief theory and background

The CARS theory is rather complex and in this paper only a brief overview will be given, for further details we refer to references cited below.

The CARS effect may be described as an interaction of two photons from one laser beam at frequency ω_p , and one photon from a laser beam at frequency ω_s through the third-order nonlinear susceptibility $\chi^{(3)}$ to generate an anti-Stokes photon at $\omega_{AS} = 2\omega_p - \omega_s$. The CARS generation can be described both classically using Maxwell's equations or quantum-mechanically utilizing the density matrix theory, e.g. as described by St. Peters [11], DeWitt et al. [12] and by Druet et al. [13].

It can be shown that the CARS intensity I_{AS} at frequency ω_{AS} may be written [14]

$$I_{AS} = \left[\frac{4\pi^2 \omega_{AS}}{c^2} \right]^2 I_p^2 I_s |\chi|_{z^2}^2 \quad (1)$$

where I_p and I_s are the laser intensities of the pump and Stokes beam, respectively, and z is the path length from which the CARS signal is generated. Following the presentation in Ref. 14, the third-order susceptibility can be divided into a resonant and a non-resonant part

$$\chi = \chi_R + \chi_{NR} \quad (2)$$

where the non-resonant part χ_{NR} , arises from electronic transitions and remote Raman transitions, and χ_R consists of one real and one imaginary part. For a Raman transitions j we thus have

$$\chi_R = \chi' + i \chi'' = \frac{2c^4}{h\omega_s^4} N \Delta_j b_j \left(\frac{d\sigma}{d\Omega} \right)_j \frac{\omega_j}{\omega_j^2 - (\omega_p - \omega_s)^2 - i\Gamma_j(\omega_p - \omega_s)} \quad (3)$$

In this equation $N\Delta_j$ is the population difference between the initial and final states, b_j is the line strength factor, $d\sigma/d\Omega$ is the Raman cross-section for the molecular species and Γ_j is the Raman linewidth. Examining Eqs. (1)-(3) several differences between CARS and spontaneous Raman scattering can be seen. Firstly, the CARS signal is highly nonlinear in both number density, laser intensity and Raman cross-section, whereas ordinary Raman scattering has a linear dependence of these factors. Secondly, the CARS process involves the population difference between the levels involved in the process, which means that $N\Delta_j$ is equal to N for low temperature and 0 for infinite temperature. Finally the CARS process also involves the Raman linewidth Γ_j . From Eqs. (2) and (3) it can be seen

$$|\chi|^2 = \chi'^2 + \chi''^2 + 2\chi'\chi_{NR} + \chi_{NR}^2 \quad (4)$$

Since χ' has a dispersive behaviour whereas χ'' has lineshape behaviour and χ_{NR} is a constant, a CARS spectrum has a complex lineshape depending on the magnitude of χ_{NR} . This can be explained according to Fig.1, which shows the behaviour for a strong weak and a line. If χ_{NR} is small, the resulting CARS lineshape is given by $\chi'^2 + \chi''^2$ and does not reveal any unusual spectral features as shown in Fig. 1a. However, if χ_{NR} is large in Eq. (4), the resulting CARS lineshape is given by

$$|\chi|^2 \sim \chi_{NR}^2 + 2\chi'\chi_{NR} \quad (5)$$

which means that the CARS resonance appears as a modulation of a background as shown in Fig. 1b. The occurrence of χ_{NR} is limiting the possibility to detect small number densities, and several approaches have been suggested to avoid this problem, e.g. by polarisation suppression [15]. When several resonances are present, as in a rotational-vibrational molecular band, the resulting CARS spectrum is further complicated through strong interactions of

neighbouring resonances and the background. Thus a computer code describing Eqs. (1)-(3) is needed to generate theoretical spectra, which can be used for evaluation of recorded spectra. As an example of computer generated CARS spectra, theoretical spectra of N_2 at different temperatures are shown in Fig. 2. The spectroscopic constants for N_2 are from Gilson et al. [16] and a dependence of Raman linewidth Γ on the rotational quantum number J as given by Hall [17] is accounted for. The occurrence of an increasingly prominent vibrational hotband, $v=1 \rightarrow v=2$, for increasing temperature is observed together with rotational lines of increasing strength. For the chosen laser linewidth only the even- J rotational lines are resolved whereas the odd J -transitions appear only at higher resolution. The difference in rotational line intensities is due to a nuclear-spin effect, accounted for by a multiplicity factor g_J included in the individual Raman cross-sections in eq. (3). For N_2 ($I(^{14}N) = 1$) g_J is 6 for even- J lines and 3 for odd- J lines. The ratio 2 results in an intensity factor of 4 due to the quadratic dependence on $\chi^{(3)}$.

The origin for the CARS process may be schematically described by an energy-level diagram as shown to the left in Fig. 3, where two photons at ω_p and ω_s beat the Raman vibration ω_R , which then is coupled to a second ω_p photon and give rise to an anti-Stokes photon at $(\omega_p - \omega_s) + \omega_p = \omega_{AS}$. In order to achieve high efficiency in the CARS process it is important to fulfil the phase-matching condition, which is illustrated to the right in Fig. 3. The simplest type of phase-matching is the collinear approach (at the top), but since the spatial resolution normally is too low with this approach, the BOXCARS approach, shown in the middle, was introduced by Eckbreth [18]. However, when probing Raman transitions with small shifts, also this technique may be troublesome. This problem was solved by the introduction of folded BOXCARS (at the bottom), where all the input laser beams are spatially separated [19-21].

Until the mid-seventies the CARS technique was limited to stationary media since a CARS spectrum was recorded when the narrow-band laser beam at ω_s was frequency tuned through the Raman resonances, i.e. when $\omega_R = \omega_p - \omega_s$. This procedure takes several minutes and thus excludes probing in non-stationary media, e.g. turbulent flames, sparks etc. However, in 1976 Roh et al. [22] showed how a single-shot CARS spectrum could be generated. This technique which is illustrated in Fig. 4 is based on the use of a broadband dye laser ($\sim 100-200 \text{ cm}^{-1}$) which covers all vibrational/rotational Raman transitions of the molecule under study. The broadband behavior of the dye laser is simply achieved, either by using a mirror instead of the grating or by using the grating in zeroth order. The CARS beam which is anti-Stokes shifted from the pump beam is thus broadband and has to be dispersed with a spectrograph and consequently detected with an optical multichannel analyzer. The spectra in Fig. 4 is an example

from measurements on N_2 . The dye-laser spectral distribution is tuned to the correct region, e.g. by changing the dye concentration. In the figure four single-shot dye-laser spectra and one single-shot corresponding CARS spectrum are shown using a 1 m spectrograph. Whereas in scanning CARS the spectral resolution of the spectra is given by the linewidth of the lasers used, the resolution in broadband CARS is given by the dispersion of the spectrograph.

III CARS Applications

III.1 Vibrational CARS

An experimental set-up for CARS spectroscopy studying vibrational Raman resonances is shown in Fig. 5. In most cases the second harmonic from a Nd:YAG laser is used both as pump beam at ω_p in the CARS process and also for pumping a dye laser which produces the Stokes laser at ω_s . The beams are arranged according to the BOXCARS configuration and focused and crossed in the flame with a lens L. The CARS beam generated from the common crossing point of the incident laser beams follows the properties of the primary laser beams. Thus, in order to recollimate the signal a second lens L is used. Since the CARS beam is generated almost collinearly with the isolated pump beam, a dichroic mirror is used to spectrally isolate the CARS beam. In Fig. 5 is shown both the set-up for scanning CARS using a photomultiplier tube and boxcar integrator and the detection scheme for broadband CARS consisting of some spectrograph and a diode-array detector (DA) connected to a multichannel analyzer. A diode array does normally consist of 512 or 1024 intensified diodes $25 \mu\text{m} \times 2.5 \text{mm}$ each, which can be gated to discriminate against continuous background, e.g. flame emission. As example of different CARS spectra of molecules of interest in combustion diagnostics Fig. 6 shows some broadband BOXCARS spectra [10]. The spectrum of O_2 is the one that resembles that of N_2 most, however, every second line in this spectrum is missing due to the nuclear spin effect ($I(^{16}O)=0, g_J=0$ for even J). Another diatomic molecule shown in the figure is H_2 . This light molecule has an extremely large rotational constant. This fact makes it easy to resolve all the individual rotational transitions in the Q-branch. The nuclear-spin-weighting factor for H_2 are 3 and 1 for odd- and even -J transitions, respectively ($I(^1H)=1/2$). This results in a nine-fold intensity alternation between rotational transitions in the H_2 CARS spectrum. The large splitting between the J-transitions makes H_2 CARS spectra well suited for temperature measurements. H_2O , being a polyatomic molecule, has a more complicated CARS spectrum than the diatomic molecules discussed so far. A recording is included in Fig. 6. Nevertheless, it has been possible to obtain excellent agreement between experimental and theoretical CARS spectra of H_2O [23]. The CARS spectrum of CH_4 , shown in the figure, is too complicated to be completely analyzed; identified is only the strong Raman-allowed transition at a shift of 2916cm^{-1} .

As was mentioned in the introduction CARS has shown to have great potential for real world applications. One of the first demonstrations of this kind was CARS experiments on a semi-industrial oil furnace [8]. A couple of years ago we initiated a project aimed at investigation of the potential for making CARS experiment in a full-scale (10 m x 10 m) industrial coal furnace [7]. For this purpose a movable CARS table was built, where collinear CARS was used for its simplicity. In order to increase the inherently bad spatial resolution with collinear CARS, a beam expander was used to increase the laser-beam diameter about a factor of three. The laser beams were then focused with a lens, $f=5\text{m}$, through an inspection hole, into the furnace. On the opposite side of the furnace, also after an inspection hole, the generated CARS beam was recollimated with a lens, $f=3\text{m}$, and detected similarly as was shown in Fig. 5. During the experiments it was evident that the large beam attenuation through the furnace (5% transmission) made it impossible to make any broadband experiments because of consequent low signal intensity. Therefore the dye laser was used narrowband ($\sim 0.4\text{ cm}^{-1}$) and then a CARS signal was clearly detected using a photomultiplier tube and a gated integrator. In Fig. 7 is shown a schematic view of the experimental set-up. The nine coal fired burners produce in total 150 MW of heat. In the figure is also inserted a CARS spectrum of N_2 molecules, taken from the boiler b), whereas a) shows a computer generated CARS spectrum at 900K for comparison. Clearly, it is not quite adequate to make a scanning recording in a temperature fluctuating medium since a cool contribution to the CARS signal will be weighted stronger than a warm one. In order to get a true temperature and to build up a temperature p.d.f. (probability distribution function) based on several single-shot spectra, it is necessary to achieve the temperature information in a single laser pulse. One way to achieve this in a low signal-intensity situation is presented in Refs. 24 and 25. This technique is based on the use of a dye laser emitting only two narrow-band wavelengths instead of a broad wavelength distribution. The two-color dye laser is achieved by using a wedge in the dye-laser cavity as shown in Fig. 8 [24]. With a proper wedge, which covered half of the expanded laser beam in the cavity, it was possible to get a dye-laser beam with wavelengths centered at the fundamental band and hot band in N_2 , i.e. approximately seven Ångström apart. The apparent advantages with the two-color CARS approach is thus; 1) higher signal strength since the dye-laser power is brought into only two components (the signal increase is about a factor of thirty.) 2) The temperature can be determined much faster than if a complete fitting procedure is used. This is of special interest when probing in turbulent media where several single-shot CARS spectra have to be used in order to build up pdf's. 3) It is possible to use photomultiplier tubes instead of diode-array detectors, which are much cheaper and probably have higher sensitivity. The disadvantage with the technique is that since only two components are being analyzed, the temperature accuracy is

expected to be somewhat lower. We have made preliminary tests of the accuracy by measuring 1000 single shot temperatures in a laminar steady flame. The standard deviation of the temperature was $\sim 80\text{K}$, whereas the same figure using a broadband dye-laser and a complete regression analyses is $\sim 50\text{K}$. However, by using a correct referencing scheme, e.g. as described in Ref. 26 the number should be possible to decrease further.

Another area in which the CARS technique is very attractive is in probing in electrical discharges and sparks. Here the possibility to measure both rotational and vibrational temperatures is of great importance since these are not necessarily the same. An example of a CARS spectrum of N_2 in a DC electrical discharge is shown in Fig. 9 [10]. Comparing this spectrum with those shown in Fig. 2 it is clearly evident that non-thermal equilibrium prevails. The rotational temperature is rather low, $\sim 450\text{K}$, whereas the vibrational temperature is much higher $\sim 2800\text{K}$.

III.2 Rotational CARS

So far only CARS measurements using vibrational Raman transition have been described. However, it is also possible to use pure rotational transition for diagnostic purposes. The advantage with rotational CARS is that several species can be measured using only one single dye laser. Since the rotational transitions are normally separated with several wavenumbers it is also very easy to interpret the spectra, even without using a sophisticated computer code as was described above for vibrational CARS. Historically the main disadvantage with rotational CARS was the difficulty to spectrally isolate the signal from the primary laser beams which were separated only some tens of wavenumbers and of course several orders of magnitude stronger than the CARS beam. The first demonstration of pure rotational CARS was on H_2 molecules [27]. However, due to the large rotational constant of this molecule the laser interferences were not too troublesome. The breakthrough came when the folded BOXCARS concept was introduced [19-21]. Here it was possible to spatially separate the rotational CARS beam from the laser beams and thus achieve a rotational CARS spectra free from interferences from the primary laserbeams. In Fig. 10 is shown rotational CARS spectra of N_2 , at the top in room air, and at the bottom from a flame ($\sim 2000\text{K}$). It is evident that the spectrum is broadened and that the peak intensity is shifted towards higher J-quantum numbers as the temperature is increased. The spectra in Fig. 10 were achieved by scanning the dye laser. In this case the frequency doubled output at 532 nm was used as pump beam, as in vibrational CARS, whereas the third harmonic at 355 nm is pumping the dye laser with coumarin 500 as dye. Unfortunately coumarine dyes are rather poor what regard efficiency, stability and spectral noise, which has limited the use of rotational CARS, although rotational CARS experiments using an excimer laser pumping two dye lasers has also been reported [28].

Very recently a new technique has been proposed for generation of rotational CARS spectra which eliminates many of the previous problems [29,30]. This new technique, called rotational dual broadband CARS, utilizes one narrowband green laser at 532 nm and one broadband dye-laser beam split into two components and centered at an arbitrary wavelength. The principle for this technique can be described by looking at Fig. 11. One can see that a rotational Raman excitation is beaten by two photons, one from each broadband dye-laser beam so that each Raman transition is driven by an infinite number of frequency-difference pairs all equal to the specific rotational Raman transition. Once driven, the Raman excited vibration is coupled to a photon from the green beam at 532 nm thus producing a rotational CARS component in the vicinity of the pump beam. By looking at the phase-matching diagram for this CARS technique it is evident that a planar BOXCARS approach can be used where the rotational CARS beam is generated collinearly with one of the dye-laser beams. Since the wavelength of this beam can be chosen arbitrarily it is possible to spectrally isolate the CARS beam by a simple dichroic mirror as in vibrational CARS. In Fig. 12 is shown a single shot rotational CARS spectrum of O₂ molecules at room temperature. An advantage with this technique is that each Raman component is a result of several frequency pairs from the dye laser, thus even in single shot an averaging effect does occur which will lower the noise and thus increase the temperature accuracy. Another advantage is of course that very stable and highly efficient rhodamine dyes can be used. An interesting feature with this technique is also that by using one additional green beam, i.e. in total four beams two green and two red, it is possible to produce simultaneously rotational and vibrational CARS spectra [30]. In this case a double folded BOXCARS approach is used and the dye laser is centered where the vibrational Raman resonance is, i.e. $\omega_S = \omega_P - \omega_R$. For N₂ this means that rhodamine 640 is used as dye and centered at 607 nm. This new technique for producing rotational CARS spectra has also been used for measurements in flame environment and these results as well as accuracies and detailed comparisons with vibrational CARS and conventional rotational CARS will be presented elsewhere [31].

IV Summary

As has been described the CARS technique has a considerable potential for diagnostic purposes in different high-temperature environment. The features as being a coherent process producing the signal as a new laser beam, the large signal strength, the non-intrusiveness and to yield high spectral, spatial and temporal resolution are of considerable advantage in all kinds of applications.

Of special current interest in terms of CARS accuracy is the question of CARS noise, both for resonant and non resonant gases when using single and multimode YAG lasers. Several experimental and theoretical investigations have been made in this field, see e.g. Refs. 26, 32-34. Another field of interest is high-pressure applications, e.g. for the automobile industry. The problems in this field are the pressure induced effects that affect the spectral shapes, e.g. motional narrowing.

With the same slope of achievement in the future as has been in the past years, it is most probable that the CARS technique will be a tool that might be useful also outside the laboratory, e.g. for control and steering of industrial processes.

Acknowledgement

The author acknowledge many stimulating discussions and fruitful cooperation with colleagues at our department. This work was financially supported by the Swedish Board for Technical Developments, STU, the National Swedish Energy Board, STEV, and AB Sydkraft.

References

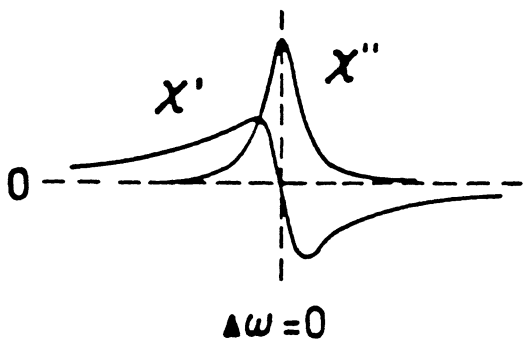
1. P.D. Maker and R.W. Terhune, Phys. Rev. A 137, 801 (1965).
2. P.R. Regnier and J.P.E. Taran, Appl. Phys. Lett. 23, 240 (1973).
3. A.C. Eckbreth, G.M. Dobbs, J.H. Stufflebeam, and P.A. Tellex, Appl. Opt. 23, 1328 (1984).
4. D.A. Greehalgh, F.M. Porter, and W.A. England, Combust. Flame 49, 171 (1983).
5. D. Klick, K.A. Marko, and L. Rimai, Appl. Opt. 20, 1178 (1981).
6. L.P. Goss, D.D. Trump, B.G. MacDonald, and G.L. Switser, Rev. Sci. Instrum. 54, 563 (1983).
7. M. Aldén and S. Wallin, Appl. Opt. 24, 3434 (1985).
8. A. Ferrario, M. Garbi, and C. Malvicini, Techn. Digest, Conf. on Lasers and Electro-Optics (Opt. Soc. of America, 1983) paper WD2.
9. E.J. Beiting, Appl. Opt. 25, 1684 (1986).
10. M. Aldén, H. Edner and S. Svanberg, Physica Scripta 27, 29 (1983).
11. R.L. St. Peters, General Electric Corporate Res. and Dev., Reports 78CRD220 and 78CRD249 (1978).
12. R.W. DeWitt, A.B. Harvey and W.M. Tolles, NRL Memorandum Report, No 3260 (1976).
13. S. Druet and J.P. Taran, Prog. Quant. Electr. 7, 1 (1981).
14. A.C. Eckbreth, P.A. Bonczyk, and J.F. Verdieck, Progress in Energy and Combustion Science, 5, 253 (1979).
15. L.A. Rahn, L.J. Zych and P.L. Mattern, Opt. Comm. 30, 249 (1974).
16. T.R. Gilson, I.R. Beattie, J.D. Black, D.S. Greenhalgh and S.N. Jenny, J. Raman spectr. 9, 361 (1980).
17. R.J. Hall, Appl. Spectr. 34, 700 (1980).
18. A.C. Eckbreth, Appl. Phys. Lett. 32, 421 (1978).

19. J.A. Shirley, R.J. Hall and A.C. Eckbreth, Opt. Lett. 5, 380 (1980).
20. Y. Prior, Appl. Opt. 19, 1741 (1980).
21. R.L. Farrow, P.L. Mattern and L.A. Rahn, Sandia Lab. Report SAND 80-8640 (1980).
22. W.B. Roh, P.W. Schreiber and J.P.E. Taran, Appl. Phys. Lett. 29, 174 (1976).
23. R.J. Hall and A.C. Eckbreth, Opt. Eng. 20, 494 (1981).
24. M. Aldén and S. Wallin, Appl. Opt. 23, 2053 (1984).
25. M. Aldén and S. Wallin, "A Preliminary Study of the Applicability of the CARS Technique in Industrial Combustors, through Transmission- and Two-Wavelength Experiments, Lund Reports on Atomic Physics, LRAP-44(1985).
26. S. Kröll, M. Aldén, T. Berglind and R.J. Hall, Appl. Opt. 26, 1068 (1987).
27. J.J. Barrett, Appl. Phys. Lett. 29, 722 (1976).
28. B. Dick and A. Gierulski, Appl. Phys. B40, 1 (1986).
29. A.C. Eckbreth and T.J. Anderson, Opt. Lett. 11, 496 (1986).
30. M. Aldén, P.-E. Bengtsson and H. Edner, Appl. Opt. 25, 4493 (1986).
31. M. Aldén, P.-E. Bengtsson, H. Edner, S. Kröll and D. Nilsson, To be published.
32. R.L. Farrow and L.A. Rahn, JOSA.B, 2, 903 (1985).
33. D.R. Snelling, R.H. Sawchuk and R.E. Mueller, Appl. Opt. 24, 2771 (1985).
34. S. Kröll and D. Sandell, To be published in JOSA.B.

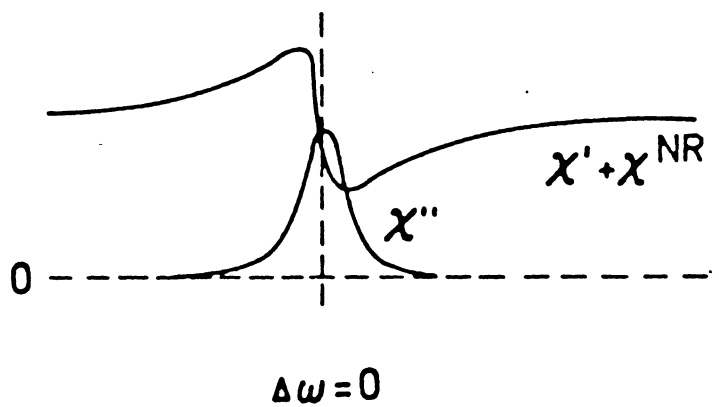
Figure Captions

1. The CARS line shape for different values of χ_R and χ_{NR} . 1a shows a strong line $\chi_R \gg \chi_{NR}$. 1b shows a weak line $\chi_R \approx \chi_{NR}$.
2. N_2 CARS spectra at different temperatures.
3. The energy level diagram describing the CARS process (to the left), and different phase-matching conditions (to the right).
4. Principle of broadband CARS
5. General CARS set-up illustrating scanning and broadband detection.
6. Broadband CARS spectra of O_2 , H_2 , H_2O and CH_4 .
7. Schematic view of the CARS experiments in a 150 MW coal fired furnace. Inserted is also an experimental and a computer generated CARS spectrum.
8. Experimental approach for producing a two-color dye laser.
9. N_2 CARS spectrum from a DC discharge.
10. N_2 Rotational CARS spectra
 - a) from room air
 - b) from a Bunsen burner flame ($T \sim 2000K$).
11. Energy level diagram illustrating the principle for rotational dual broadband CARS.
12. Single shot O_2 rotational CARS spectrum at room temperature produced using rotational dual broadband CARS.

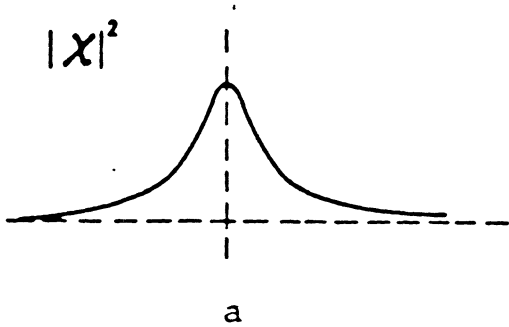
STRONG LINE



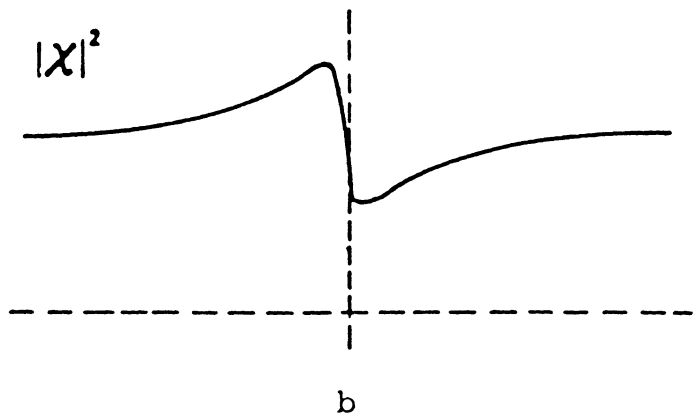
WEAK LINE

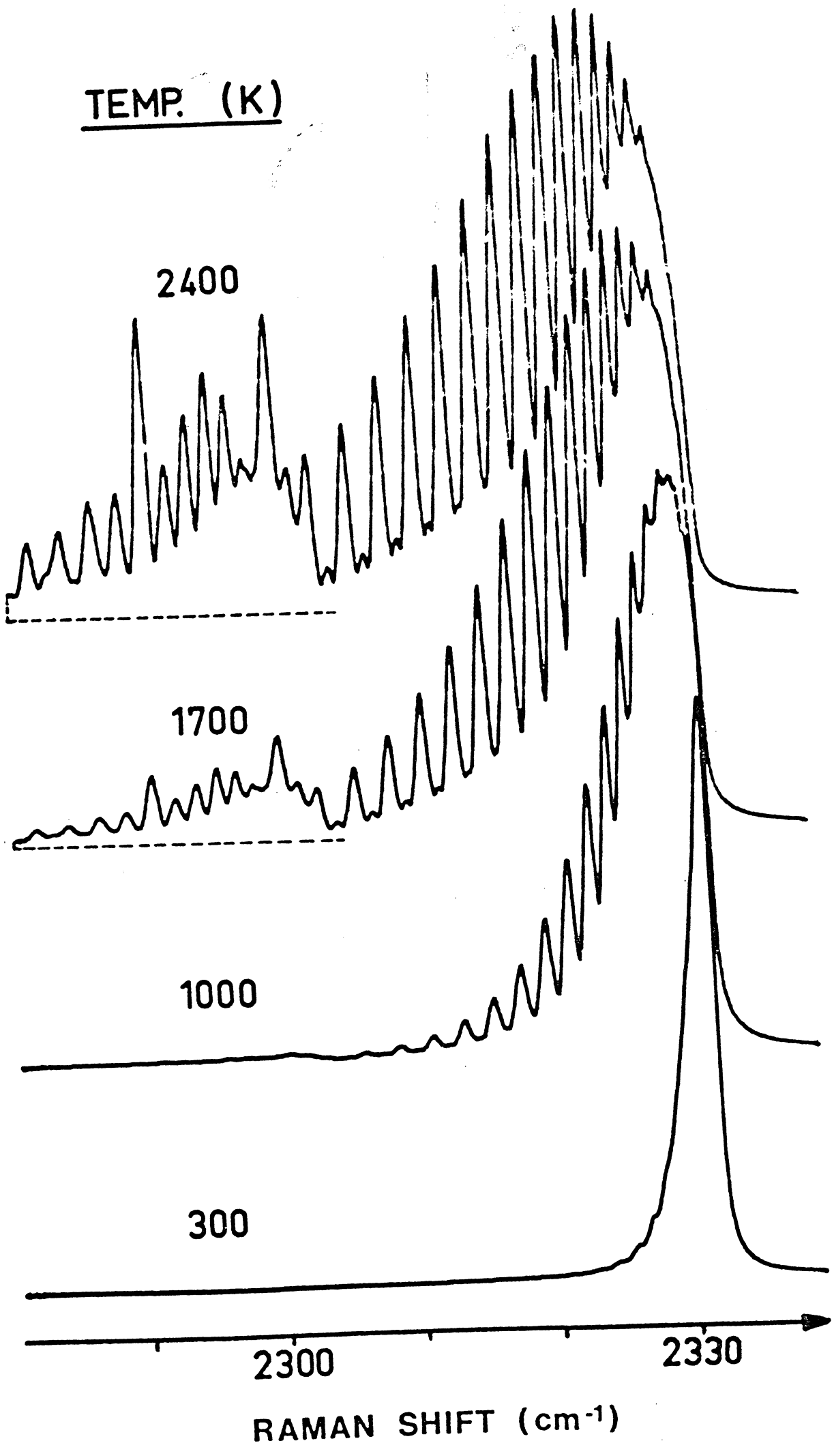


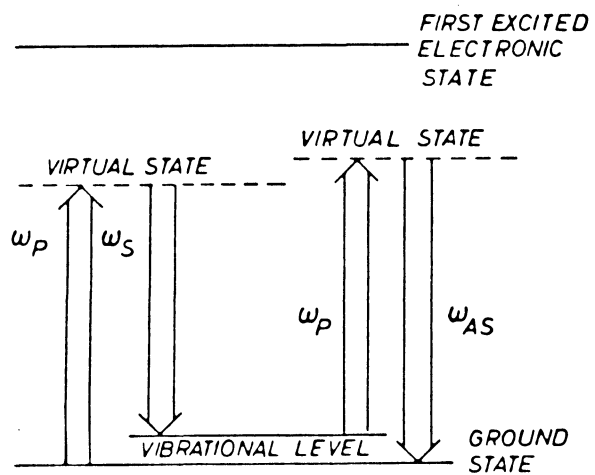
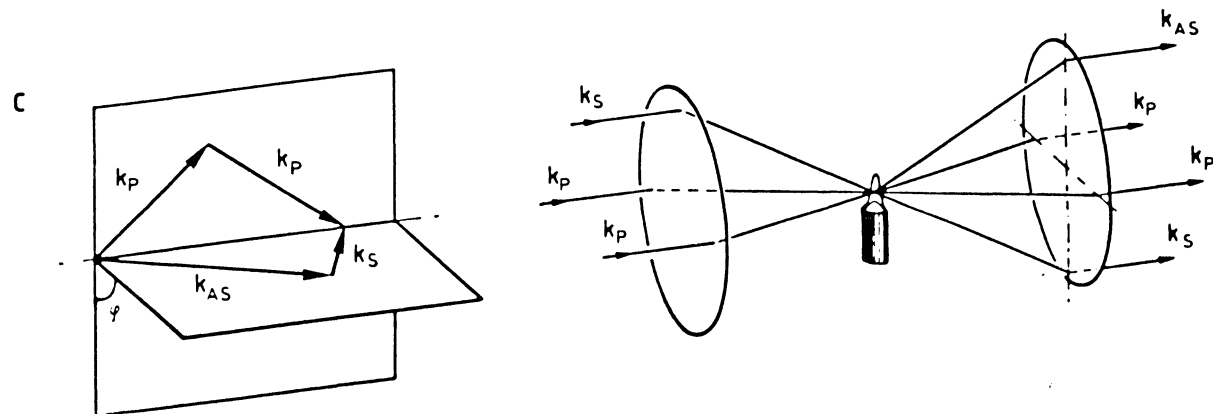
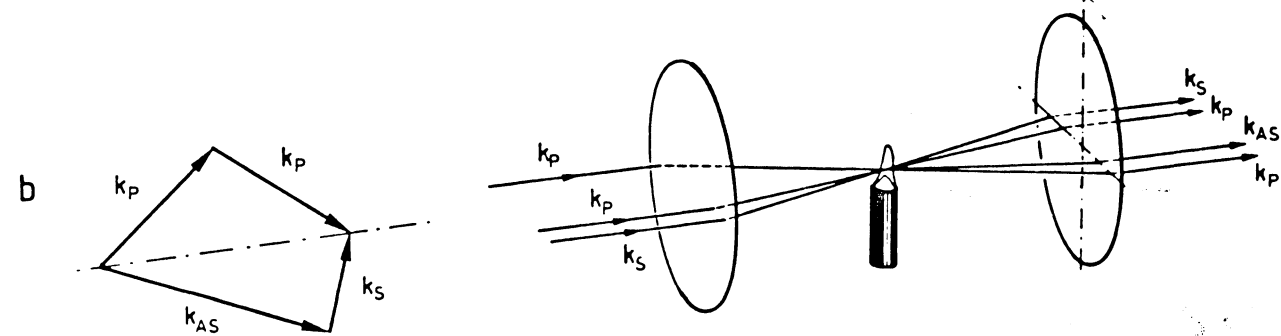
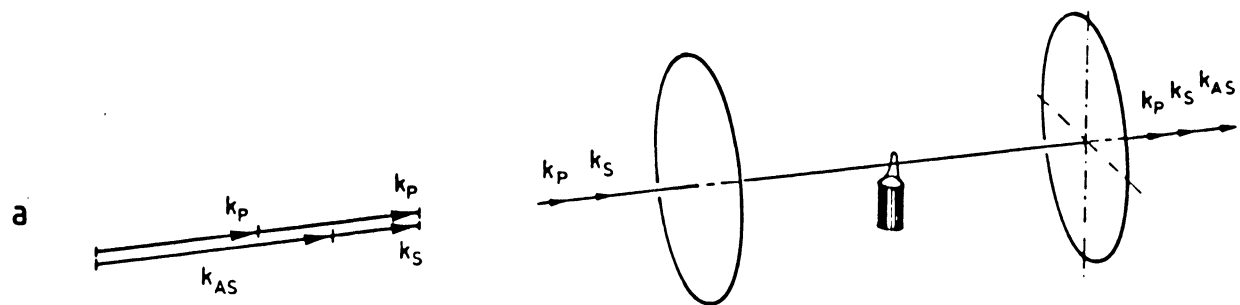
$|x|^2$



$|x|^2$







BROADBAND CARS

CARS SPECTRUM

PUMP LASER

DYE PROFILE

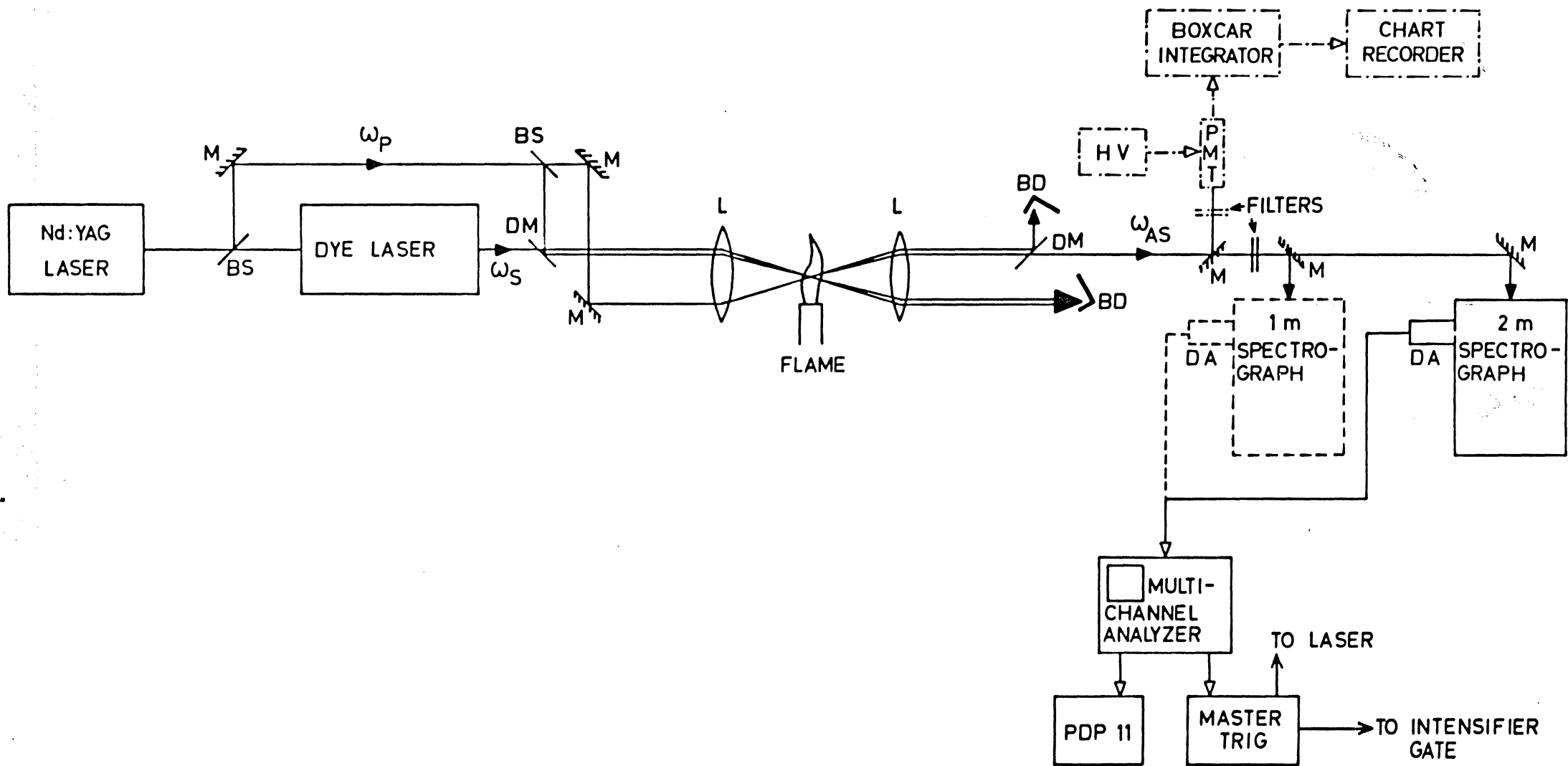
30 cm^{-1}

$$\omega_{AS} = 2\omega_P - \omega_S$$

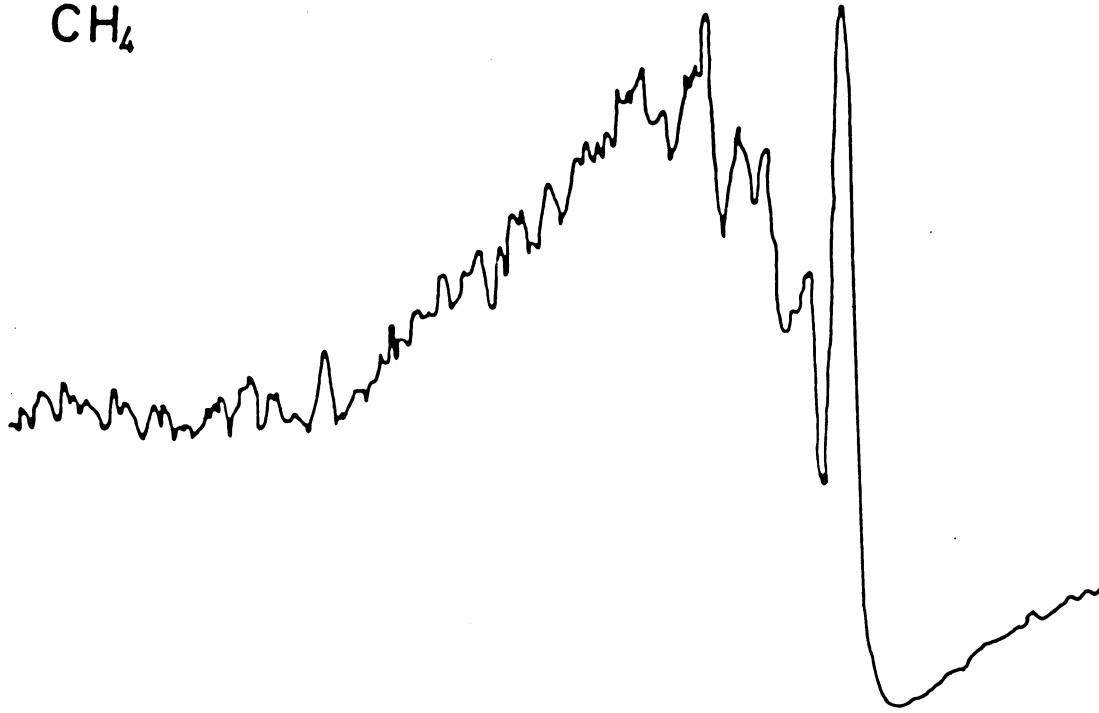
ω_P

ω_S

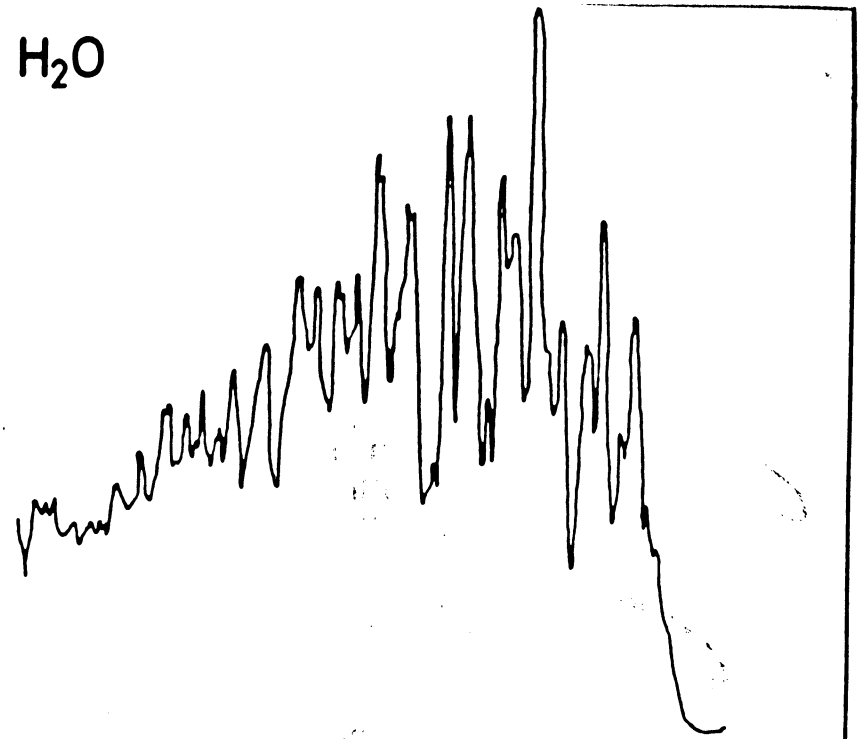
4



CH₄



H₂O



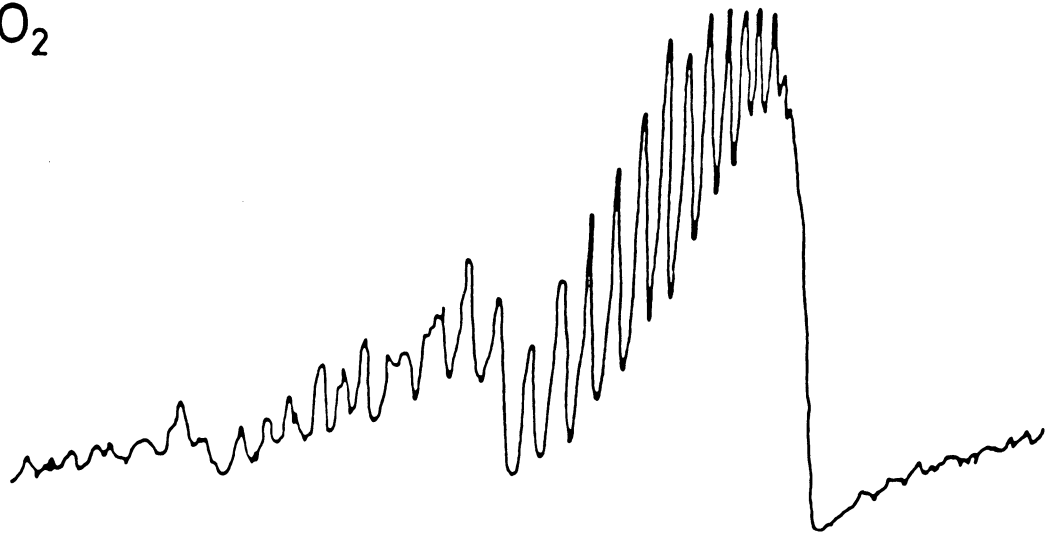
21650

21700

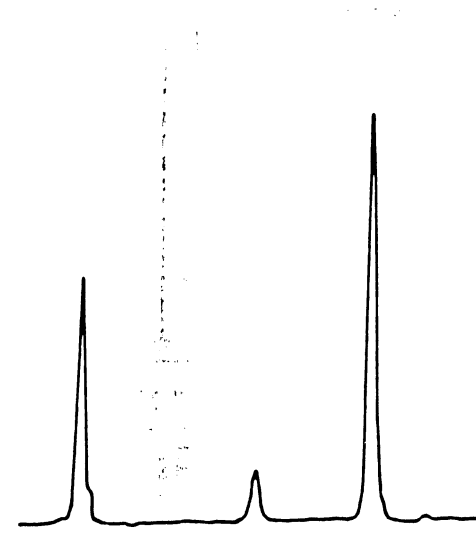
22400

22450

O₂



H₂



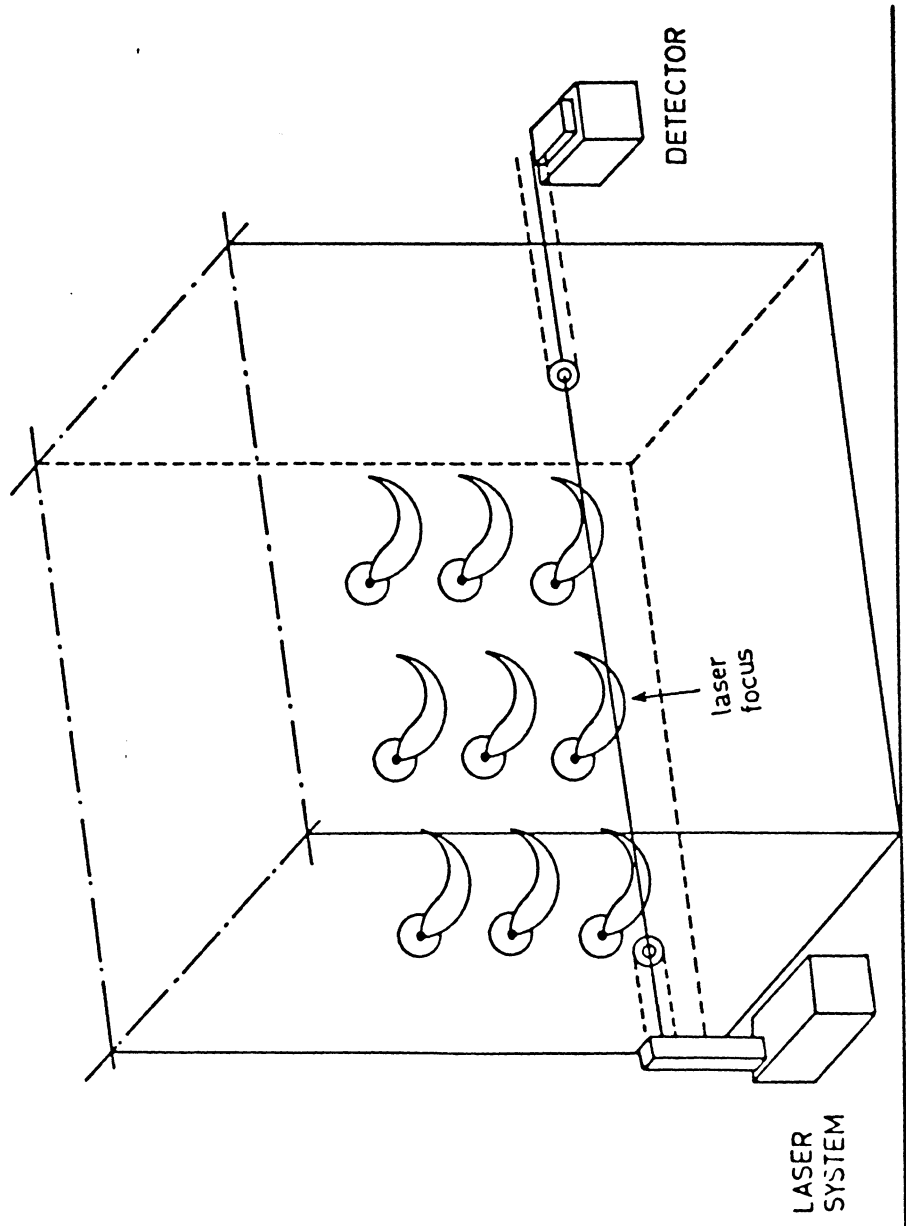
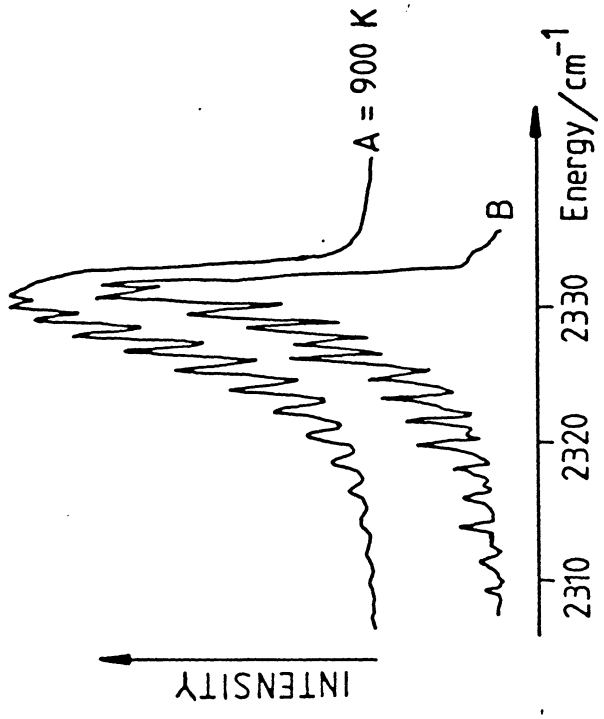
20300

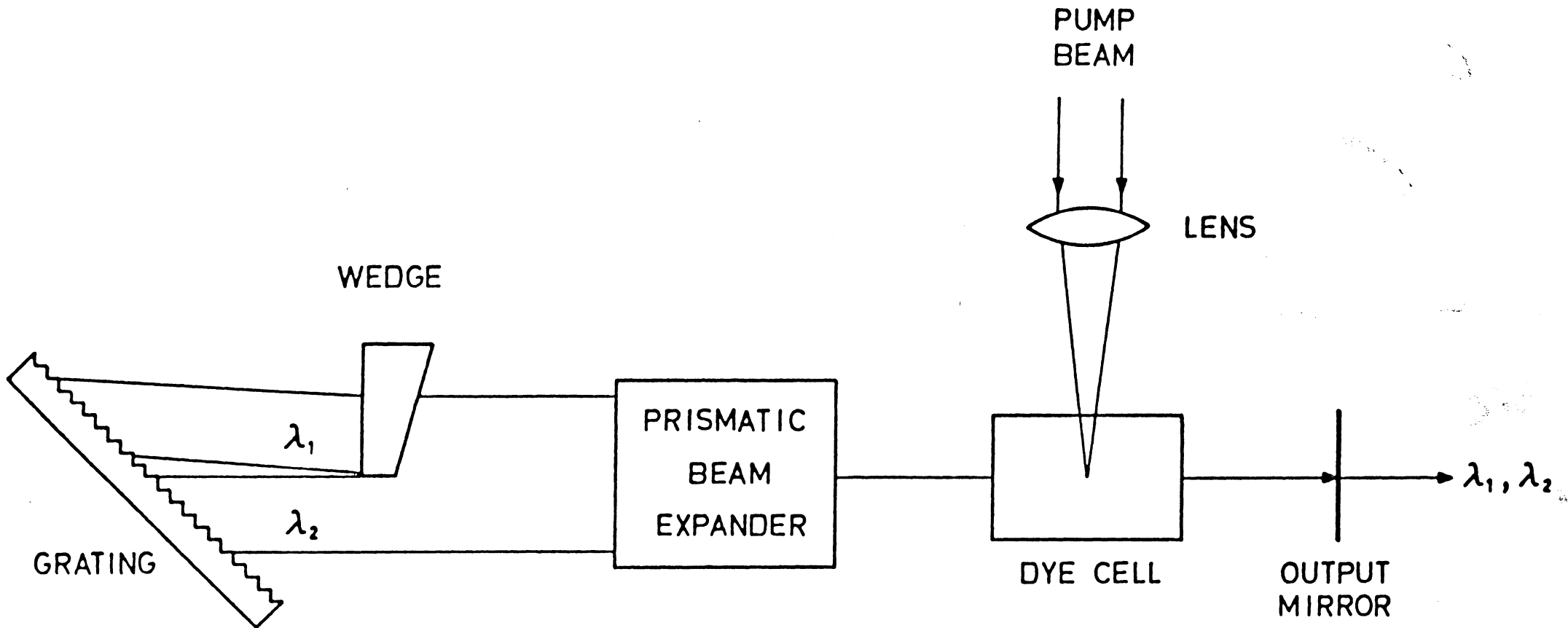
20350

22920

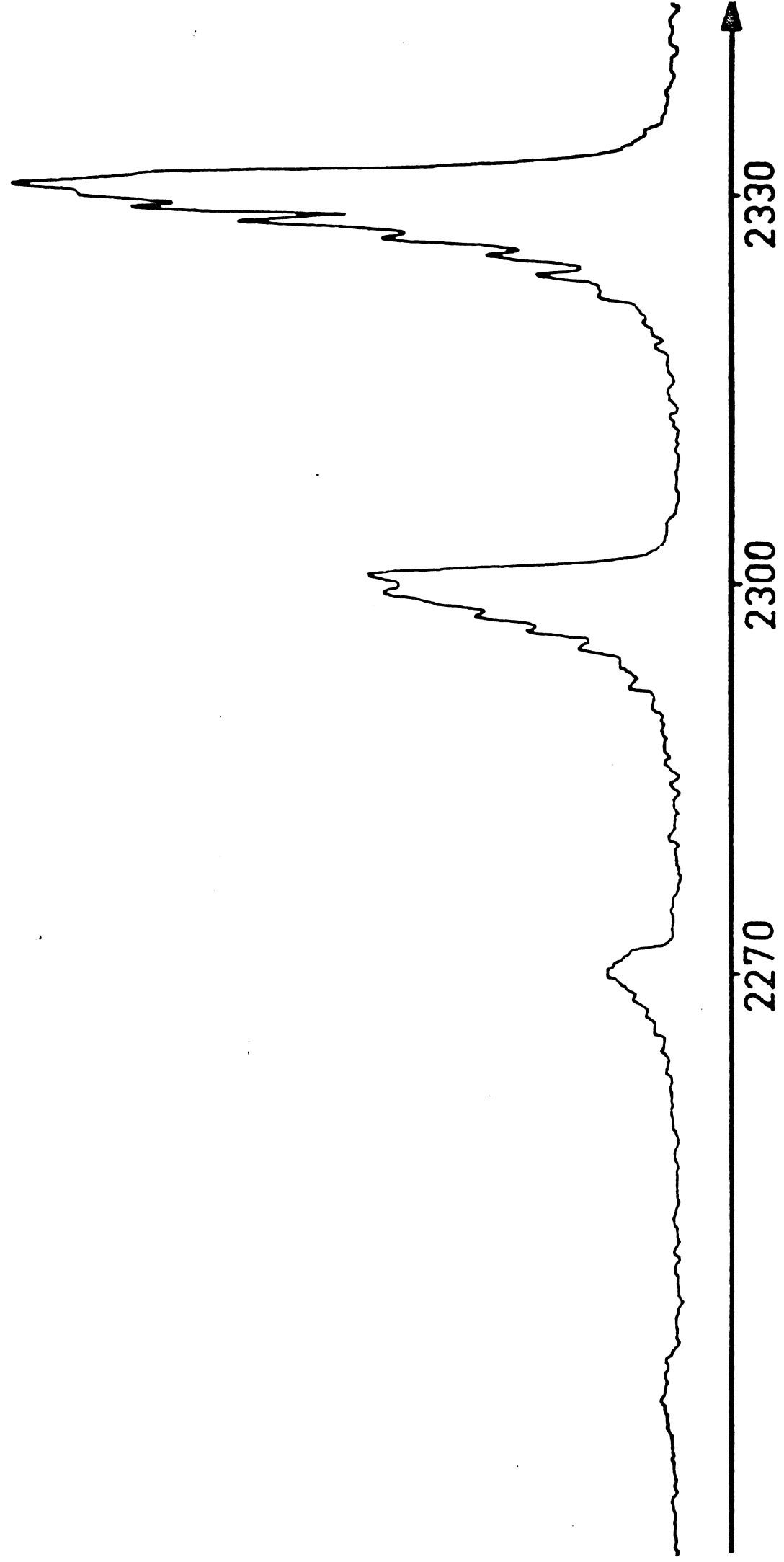
22950

FREQUENCY [cm⁻¹]





BOXCARS SPECTRUM FROM A DC DISCHARGE IN N₂



RAMAN SHIFT (cm⁻¹)

